arXiv:1704.00444v1 [hep-ph] 3 Apr 2017

Some new aspects of quarkonia production at the LHC *

Antoni Szczurek

Institute of Nuclear Physics Polish Academy of Sciences, PL-31342 Kraków
Anna Cisek

Faculty of Mathematics and Natural Sciences, University of Rzeszow, ul. Pigonia 1, 35-310 Rzeszów
Wolfgang Schäfer

Institute of Nuclear Physics Polish Academy of Sciences, PL-31342 Kraków

We discuss some different new aspects of J/ψ meson production in exclusive, semi-exclusive and inclusive processes. We finish with a short discussion of double J/ψ production. We point out some new results obtained recently by our group and discuss some open issues.

PACS numbers: 12.40.Nn,13.60.-r,13.60Le,13.85Ni,14.40Gx

1. Introduction

The J/ψ meson is interesting due to its simple structure ($c\bar{c}$ state). However, the mechanism of its production is not always well understood. There are different subfields of high energy physics that deal with the production of J/ψ meson. Our group participated in different fields and it is the aim of this talk (presentation) to show some progress in the different fields.

The first topic is connected with the exclusive production of J/ψ mesons in the $pp \to ppJ/\psi$ reaction. There the main production mechanism is a photon-pomeron fusion. The same type of process was studied some years ago in the context of $\gamma p \to J/\psi p$ reactions measured at HERA [1]. The pomeron is a key word which is understood and used by different authors often very differently. At high energies, which corresponds to small fractions of gluon longitudinal momentum fractions, a problem of gluon saturation may be important. The problem with the current experiment is that so far it was not possible to control the exclusivity of the process. Therefore

* Presented at the Epiphany 2017 conference

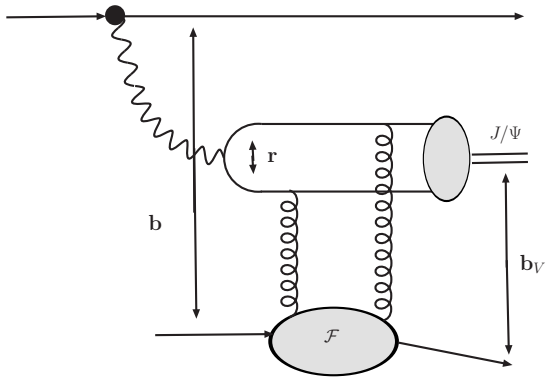


Fig. 1. A sketch of dynamics of the $\gamma p \to J/\psi p$ process.

recently we have performed more detailed studies of semiexclusive processes that contribute in experimental environment but strictly speaking are not exclusive in a rigorous sense of the word.

The inclusive production of J/ψ mesons is a long standing problem in spite that there are well formulated nonrelativistic pQCD rules. Forward production of J/ψ mesons may be also related to the phenomenon of gluon saturation. Recent years the luminosity of the running experiments was increased and allowed to measure even two J/ψ mesons in one event. Here a new mechanism, called double parton (or multiple parton) scattering, may appear at high energies, where the density of partons, in particular of gluon becomes large. In contrast to single parton scattering the formalism of double (or multiple) scattering is not under similar theoretical precision. While there was a relatively good agreement for experiments where low transverse momenta of J/ψ mesons were involved (e.g. LHCb), the cases where cuts on transverse momenta are (were) more problematic and large disagreement of theoretical calculation with the data was observed unless the constant known as effective cross section was considerably lowered. Below we wish to discuss some mechanisms that were neglected and may be important in good understanding of the situation.

2. Exclusive $pp \to ppJ/\psi$ reaction

2.1. Sketch of the theoretical methods

The imaginary part of the forward amplitude sketched in Fig.1 can be written as [1]:

$$\Im m\,\mathcal{M}_T(W,\Delta^2=0,Q^2=0) = W^2\frac{c_v\sqrt{4\pi\alpha_{em}}}{4\pi^2}\,2\int_0^1\frac{dz}{z(1-z)}\int_0^\infty \pi dk^2\psi_V(z,k^2)$$
$$\int_0^\infty\frac{\pi d\kappa^2}{\kappa^4}\alpha_S(q^2)\mathcal{F}(x_{\rm eff},\kappa^2)\Big(A_0(z,k^2)\;W_0(k^2,\kappa^2)+A_1(z,k^2)\;W_1(k^2,\kappa^2)\Big)\,, \quad (1)$$

The full amplitude, at finite momentum transfer is given by:

$$\mathcal{M}(W,\Delta^2) = (i+\rho)\,\Im m\mathcal{M}(W,\Delta^2=0,Q^2=0)\,\exp(-B(W)\Delta^2/2)\,, \quad (2)$$

where the real part of the amplitude is restored from analyticity,

$$\rho = \frac{\Re e\mathcal{M}}{\Im m\mathcal{M}} = \tan\Big(\frac{\pi}{2}\,\frac{\partial\log\Big(\Im m\mathcal{M}/W^2\Big)}{\partial\log W^2}\Big)\,. \quad (3)$$

Above $B(W)$ is a slope parameter which in general depends on the photon-proton center-of-mass energy and is parametrized in the present analysis as:

$$B(W) = b_0 + 2\alpha'_{eff}\log\Big(\frac{W^2}{W_0^2}\Big)\,. \quad (4)$$

The full Born amplitude for the $pp\to pVp$ process (see Fig.2) can be written as:

$$\mathcal{M}^{\lambda_1\lambda_2\to\lambda_1'\lambda_2'\lambda_V}_{h_1h_2\to h_1h_2V}(s,s_1,s_2,t_1,t_2) = \mathcal{M}_{\gamma I\!P}+\mathcal{M}_{I\!P\gamma}$$
$$= \langle p_1',\lambda_1'|J_\mu|p_1,\lambda_1\rangle\epsilon^*_\mu(q_1,\lambda_V)\frac{\sqrt{4\pi\alpha_{em}}}{t_1}\mathcal{M}^{\lambda_{\gamma^*}\lambda_2\to\lambda_V\lambda_2}_{\gamma^*h_2\to Vh_2}(s_2,t_2,Q_1^2)$$
$$+\langle p_2',\lambda_2'|J_\mu|p_2,\lambda_2\rangle\epsilon^*_\mu(q_2,\lambda_V)\frac{\sqrt{4\pi\alpha_{em}}}{t_2}\mathcal{M}^{\lambda_{\gamma^*}\lambda_1\to\lambda_V\lambda_1}_{\gamma^*h_1\to Vh_1}(s_1,t_1,Q_2^2)\,. \quad (5)$$

The electromagnetic transition matrix elements contain both helicity conserving and helicity flip components [2].

The effects of absorption are illustrated in Fig.3. The relevant formalism is described e.g. in Ref.[3].

2.2. Selected results

Most of the calculations in the literature neglect the anomalous photon coupling to proton quantified by the Pauli coupling. In Fig.4 we illustrate the role of the Pauli form factor on the transverse momentum distribution

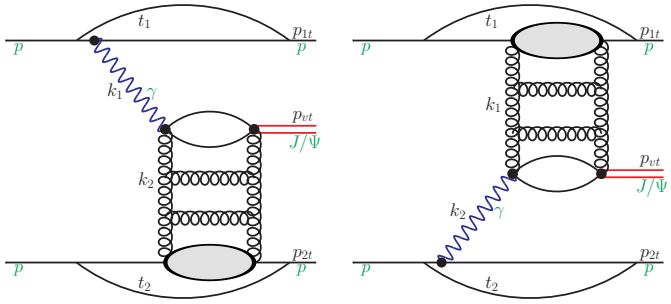


Fig. 2. Two mechanisms of exclusive J/ψ meson production at the Born level.

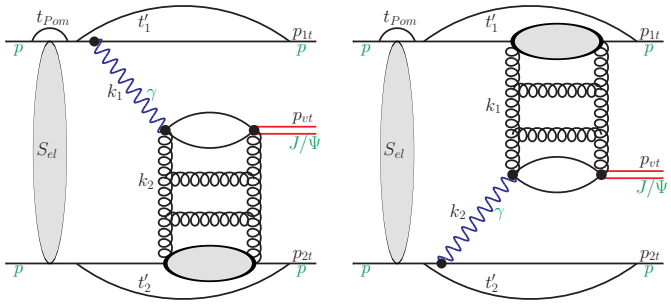


Fig. 3. A sketch of the absorption effects that lead to a decrease of the Born cross sections.

of J/ψ mesons. Inclusion of Pauli form factor considerably enhances the cross section at large transverse momenta of J/ψ meson.

In Fig.5 we show rapidity distributions for different unintegrated gluon distribution function (UGDF). The results strongly depend on UGDF used. The best result is achieved with UGDFs that include nonlinear effects (here a nonlinear Kutak-Stasto UGDF was used). This may be connected with the onset of gluon saturation, a phenomenon expected to show up in processes with small gluon longitudinal momentum fraction but never unambiguously identified.

The role of absorption effects is illustrated in Fig.6. The absorption effects modify the shape of transverse momentum distributions. Therefore a careful treatment of absorption effects is very important in the context of possible searches for odderon exchange discussed in the literature.

In Ref.[2] we have shown similar effects for ψ' meson production. Here

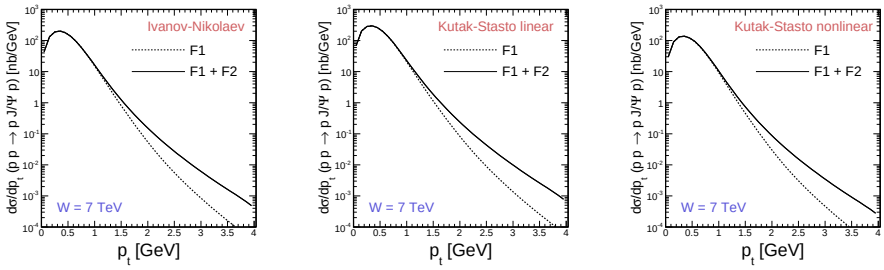


Fig. 4. Transverse momentum distributions of exclusively produced J/ψ mesons for three different unintegrated gluon distributions. We compare results with Dirac and Dirac+Pauli electromagnetic form factor.

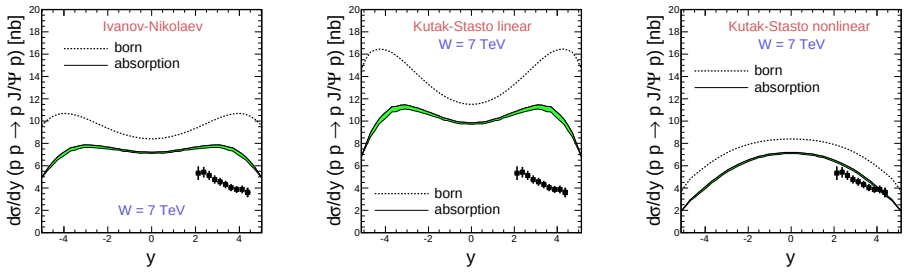


Fig. 5. Rapidity distributions of exclusively produced J/ψ mesons for three different unintegrated gluon distributions at $\sqrt{s} = 7$ TeV.

we show only the ratios of the cross section for ψ' to the cross section for J/ψ meson production as a function of J/ψ (ψ') rapidity. A good agreement is achieved for the Gaussian wave functions. In contrast, approaches that do not use wave functions cannot give a reasonable description of the data.

3. Semiexclusive production of J/ψ mesons with proton dissociation

3.1. Sketch of the theoretical methods

There are a few mechanisms of semiexclusive excitation of participating protons. Let us start from electromagnetic dissociation of one of the protons (see Fig.8).

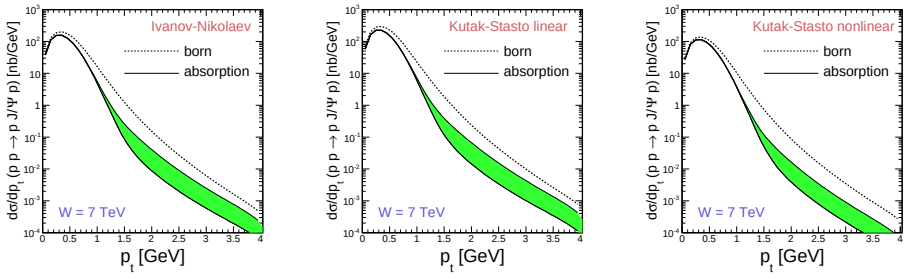


Fig. 6. Transverse momentum distributions of exclusively produced J/ψ mesons for three different unintegrated gluon distributions.
The shaded (green online) band represents typical uncertainties in calculating absorption effects as described in the text.

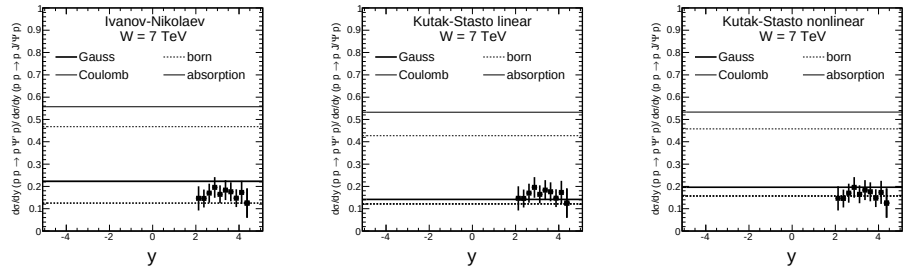


Fig. 7. The ratio of the cross section for ψ' to that for the J/ψ meson.

The cross section for such processes can be written as:

$$\frac{d\sigma(pp\to XVp;s)}{dyd^2\mathbf{p}dM_X^2}=\int\frac{d^2\mathbf{q}}{\pi\mathbf{q}^2}\mathcal{F}^{(\mathrm{inel})}_{\gamma/p}(z_+,\mathbf{q}^2,M_X^2)\frac{1}{\pi}\frac{d\sigma^{\gamma^*p\to Vp}}{dt}(z_+s,t=-(\mathbf{q}-\mathbf{p})^2)$$
$$+(z_+\leftrightarrow z_-), \tag{6}$$

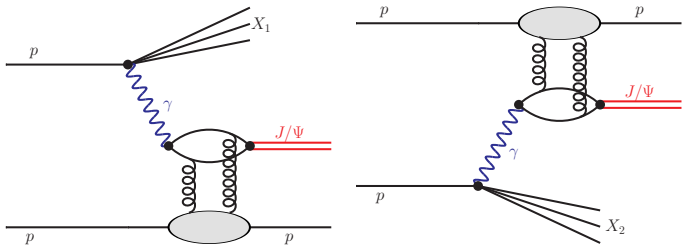


Fig. 8. Electromagnetic excitation of one of the photons in proton-proton collisions.

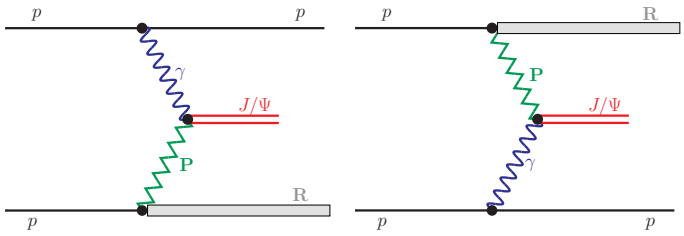


Fig. 9. Diffractive excitation of resonances on one of the protons.

where $z_\pm = e^{\pm y}\sqrt{(\mathbf{p}^2+m_V^2)/s}$. In the kinematics of interest the "fully unintegrated" flux of photons associated with the breakup of the proton is calculable in terms of the structure function F_2 of a proton [5, 6]:

$$\mathcal{F}^{(\rm inel)}_{\gamma/p}(z,\mathbf{q}^2,M_X^2) = \frac{\alpha_{\rm em}}{\pi}(1-z)\theta(M_X^2-M_{\rm thr}^2) \times \frac{F_2(x_{Bj},Q^2)}{M_X^2+Q^2-m_p^2}\Big[\frac{\mathbf{q}^2}{\mathbf{q}^2+z(M_X^2-m_p^2)+z^2m_p^2}\Big]^2 . \quad (7)$$

In distinction to electromagnetic dissociation, the diffractive excitation is highly model dependent. We consider two mechanisms of the diffractive dissociation: resonance production and continuum excitation. A diagrammatic sketch of the reaction mechanism is shown in Fig.9.

The contribution of three positive-parity baryon resonances on the nucleon trajectory are taken into account:

1. N(1680), $J=\frac{5}{2}$,
2. N(2220), $J=\frac{9}{2}$,
3. N(2700), $J=\frac{13}{2}$.

They contribute to the $p\mathbb{P}\to X$ amplitude as:

$$\Im m A(M_X^2,t) = \sum_{n=1,3}[f(t)]^{2(n+1)}\cdot\frac{\Im m\,\alpha(M_X^2)}{(J_n-\Re e\,\alpha(M_X^2))^2+(\Im m\,\alpha(M_X^2))^2}. \quad (8)$$

Here J_n is the spin of the nth resonance, and the explicit form of the complex Regge trajectory $\alpha(M_X^2)$ as well as the form factor $f(t)$ (see [10, 11]).

In addition we include the so-called Roper resonance $N^*(1440)$. More details are given in our original paper [9].

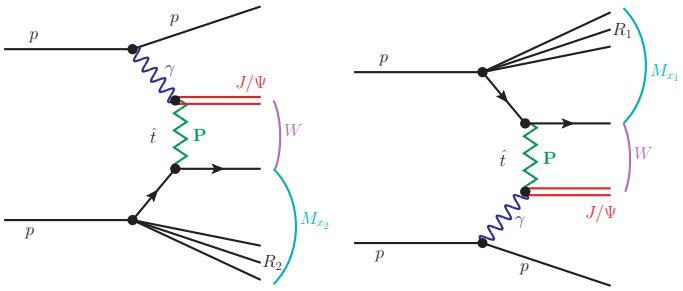


Fig. 10. Diffractive excitation of partonic continuum on one of the protons.

We include also the partonic continuum for the $\gamma p \to VX$ subreaction. Corresponding schematic diagrams are shown in Fig.10.

In this approximation the cross section can be written as

$$\frac{d\sigma^{diff,partonic}_{pp\to Vj}}{dy_V dy_j d^2p_t} = \frac{1}{16\pi^2\hat{s}^2} x_1 q_{\rm eff}(x_1,\mu_F^2) x_2 \gamma_{el}(x_2) \overline{|\mathcal{M}_{q\gamma\to Vq}|^2} + \frac{1}{16\pi^2\hat{s}^2} x_1 \gamma_{el}(x_1) x_2 q_{\rm eff}(x_2,\mu_F^2) \overline{|\mathcal{M}_{q\gamma\to Vq}|^2} \ . \quad (9)$$

We neglect transverse momenta of the photon and the initial parton. The two terms correspond to the two diagrams in Fig.10. The effective parton distribution means:

$$q_{\rm eff}(x,\mu_F^2) = \frac{81}{16} g(x,\mu_F^2) + \sum_f \left[q_f(x,\mu_F^2) + \bar{q}_f(x,\mu_F^2) \right] \ . \quad (10)$$

In Ref.[9] we use a simple formula for two-gluon exchange:

$$\frac{d\sigma_{\gamma q\to Vq}}{d\hat{t}} \propto \alpha_s^2(\bar{Q}_t^2)\alpha_s^2(|\hat{t}|) \frac{m_V^3 \Gamma(V\to l^+l^-)}{(\bar{Q}_t^2)^4} \ , \quad (11)$$

where $\bar{Q}_t^2 = m_V^2 + |\hat{t}|$. The normalization constant has been adjusted in [9] to the H1 HERA experimental data.

3.2. Selected results

In Ref.[9] we have shown many results for both full phase space as well as for particular experiments. In Fig.11 we show the distribution in rapidity of the J/ψ meson.

In Fig.12 we show transverse momentum distribution of J/ψ meson for $M_X < 5$ GeV. The larger masses of the proton excitations the larger slopes

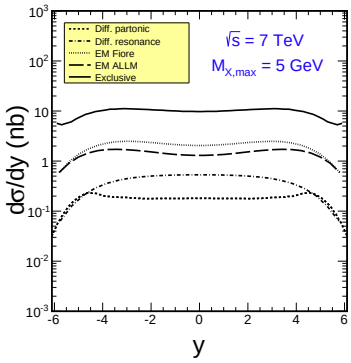


Fig. 11. Rapidity distribution of J/ψ mesons for $\sqrt{s} = 7$ TeV for purely exclusive process and for different contributions to semiexclusive processes.

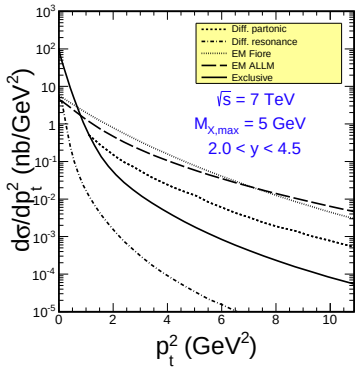


Fig. 12. Dependence of the cross section on transverse momentum squared for the LHCb experiment.

of the transverse momentum distribution of J/ψ. For comparison we show distribution for the purely exclusive case. The inelastic contributions start to dominate over the purely elastic (exclusive) contribution for $p_T > 1$ GeV.

It is also interesting to see how the cross sections for semiexclusive processes compare to those for the purely exclusive one. To quantify their contribution we define the following ratio:

$$R(y) \;=\; \frac{d\sigma_{pp\to pJ/\psi X}(M_X < M_{X,\max})/dy}{d\sigma_{pp\to pJ/\psi p}/dy} \,. \tag{12}$$

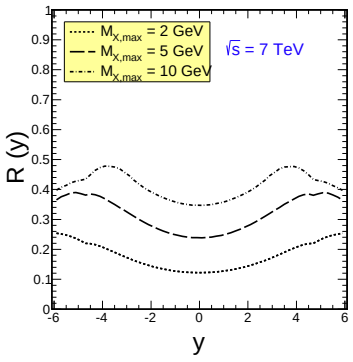


Fig. 13. The ratio of the semiexclusive-to-exclusive cross section as a function of rapidity of J/ψ meson for different ranges of proton excitation energies.

This ratio is shown in Fig.13 for three different values of $M_{X,\max}$. We see that the magnitude as well as the shape of the ratio depends on the range of missing masses included in the calculation.

4. Inclusive production of J/ψ mesons

4.1. Sketch of the theoretical methods

We now turn to the fully inclusive production of J/ψ mesons. In this presentation we shall consider only the contributions of the color-singlet mechanism. Here at the perturbative stage of the process a $c\bar{c}$ system is produced in the color-singlet state. In Figs.14 we show two dominant color-singlet mechanisms of J/ψ meson production. The first diagram represents so-called direct contribution, while the second diagram represents an example of feed down from other quarkonia.

$$\frac{d\sigma(pp\to J/\psi g X)}{dy_{J/\psi}dy_g d^2p_{J/\psi,t}d^2p_{g,t}} = \frac{1}{16\pi^2\hat{s}^2}\int \frac{d^2q_{1t}}{\pi}\frac{d^2q_{2t}}{\pi}\overline{|\mathcal{M}^{off-shell}_{g^*g^*\to J/\psi g}|^2}$$
$$\times\ \delta^2\left(\vec{q}_{1t}+\vec{q}_{2t}-\vec{p}_{H,t}-\vec{p}_{g,t}\right)\mathcal{F}_g(x_1,q_{1t}^2,\mu_F^2)\mathcal{F}_g(x_2,q_{2t}^2,\mu_F^2)\ . \qquad (13)$$

The corresponding matrix element squared for the $gg\to J/\psi g$ is proportional to the radial wavefunction at the origin:

$$|\mathcal{M}_{gg\to J/\psi g}|^2 \propto \alpha_s^3|R(0)|^2\ . \qquad (14)$$

In our calculations the matrix elements obtained by S. Baranov [8] was used.

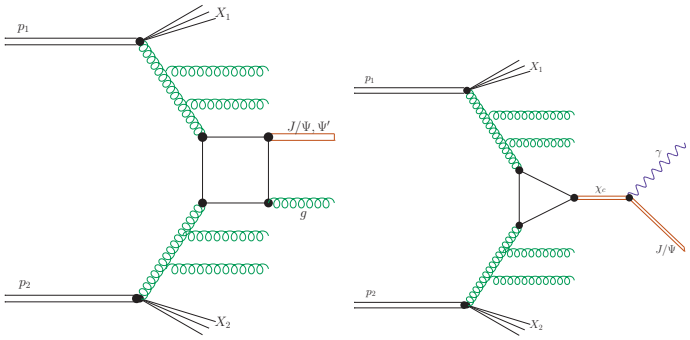


Fig. 14. Dominant color-singlet mechanisms of J/ψ meson production. The initial state gluon emissions are shown explicitly.

Another important mechanism is the production of χ_c mesons and its subsequent decay $\chi_c \to J/\psi + \gamma$. The χ_c mesons are p-wave $c\bar{c}$ states of positive C-parity. They can be produced by the gluon-gluon fusion mechanism. In the k_t-factorization approach the leading-order cross section for the χ_c meson production can be written in a similar way as the for the J/ψ production.

The matrix element squared for the $g^*g^* \to \chi_c$ subprocess is proportional to the derivative of the wave function at the origin:

$$|\mathcal{M}_{g^*g^*\to\chi_c}|^2 \propto \alpha_s^2 |R'(0)|^2 \; . \tag{15}$$

$R'(0)$ can be treated as a free parameter to get correctly relative contribution of J/ψ from χ_c. We used the matrix element taken from [12].

Another mechanism which we take into account is the production of ψ' meson and its decay. The corresponding ratio $\mathrm{Br}(\Psi' \to \mathrm{J}/\psi + \mathrm{X}) = 0.574$ is relatively large. The cross section for production of ψ' mesons is calculated using a formula analogous to Eq.(13). Of course, then the wave function of J/ψ is replaced by a wave function of ψ': $|R_{\Psi'}(0)|^2 \approx 5/8 |R_{J/\psi}(0)|^2$. The difference may be understood qualitatively as due to the fact that ψ' is a 2S state while J/ψ is 1S state (different radial excitations).

4.2. Selected results

Here we show only some selected results. More detailed discussion will be presented elsewhere [7]. In Fig.15 we show rapidity distributions obtained with the KMR UGDF. This gluon distribution gives a relatively good description of the open charm inclusive production and correlations. At low energies relatively good agreement is obtained. When increasing energy the

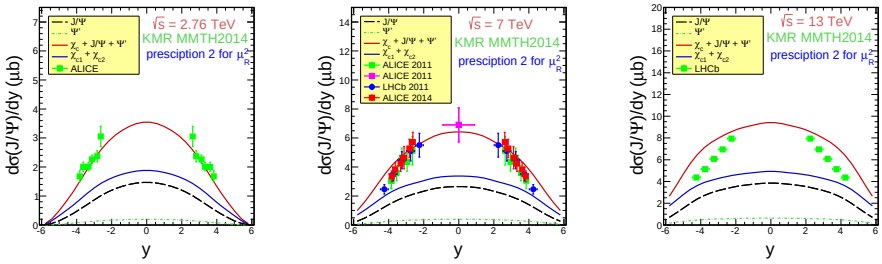


Fig. 15. Inclusive rapidity distributions of J/ψ mesons for three different energies obtained with the KMR UGDFs.

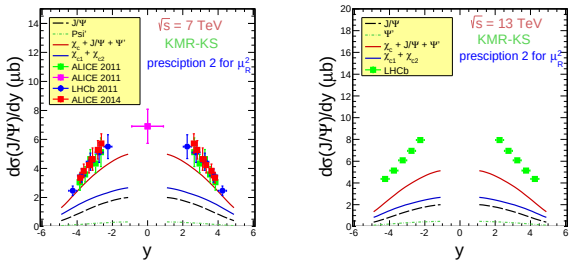


Fig. 16. Inclusive rapidity distributions of J/ψ mesons for two energies obtained with one KMR and one KS(nonlinear) UGDF.

agreement becomes worse and worse. The disagreement may be connected with the onset of nonlinear effects, leading eventually to gluon saturation which is an asymptotic (small-x) notion.

For the LHCb configuration typically one longitudinal momentum fraction is small and the other much larger. Replacing the KMR UGDF by the Kutak-Stasto UGDF for the low-x values improves the situation. In our opinion it seems precocious to draw too definite conclusion in the moment.

In [7] we will discuss many other aspects of J/ψ meson production.

5. Production of two J/ψ mesons

5.1. Sketch of the theoretical methods

The color-singlet mechanisms used so far in the literature are shown in Fig.17. The first type of diagrams will be called here "box" for brevity. The circle inside the box represents different gluon insertions. There are 20 diagrams (see e.g.[15]). These contributions are of the order of $O(\alpha_s^4)$.

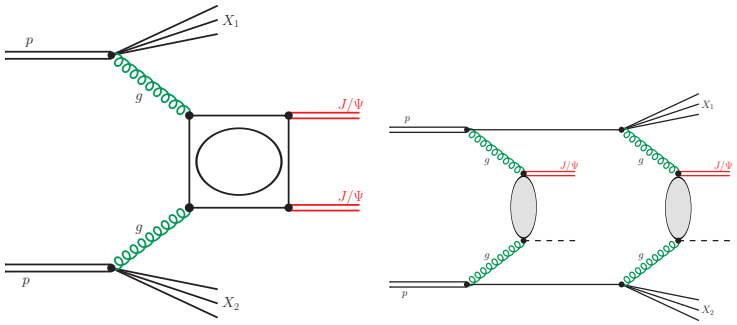


Fig. 17. Schematic representation of main mechanisms considered so far in the literature.

In addition they depend on the value of the wave function at the origin $\sigma \propto |R(0)|^4$. The matrix elements are too complicated to be shown here explicitly. The second diagram, of the order of $O(\alpha_s^6)$ represents double parton scattering mechanism. Although higher order than the previous box contributions it may be enhanced by higher powers of gluon distributions.

For the presentation at the Epiphany 2017 workshop the box contribution was calculated only in the collinear approach. [1] Then the inclusive differential cross section can be written as:

$$\frac{d\sigma(pp \to J/\psi J/\psi}{dy_{V_1} dy_{V_2} d^2p_t} = \frac{1}{16\pi^2 \hat{s}^2} \overline{|\mathcal{M}^{on-shell}_{gg\to J/\psi J/\psi}|^2} \times \; g(x_1, \mu_F^2) g(x_2, \mu_F^2) \; . \tag{16}$$

In our calculations for the presentation we used the MSTW08 gluon distributions. We have checked that the somewhat artificial matrix element gives a good representation of experimental data for inclusive J/ψ production.

The calculation of double parton scattering is simplified. Instead of including all single scattering mechanisms discussed in the previous section we parametrize the single J/ψ production using the following formula:

$$\frac{d\sigma(pp \to J/\psi g)}{dy_{J/\psi} dy_X d^2p_t} = \frac{1}{16\pi^2 \hat{s}^2} \overline{|\mathcal{M}^{eff}_{gg\to J/\psi X}|^2} \times \; g(x_1, \mu_F^2) g(x_2, \mu_F^2) \; . \tag{17}$$

We take a parametrization of the effective matrix element by Kom-Kulesza-Stirling [14] using the MSTW08 PDF.

[1] Now a full k_t-factorization approach is available but will be not shown here.

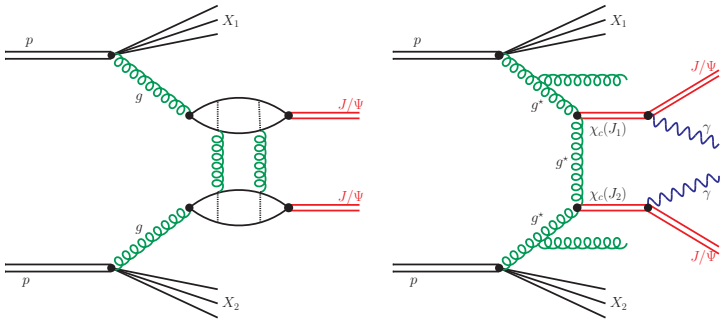


Fig. 18. New mechanisms included or being included by us recently.

In the present approach we do calculations using a factorized Ansatz. Then the cross section for double parton scattering can be written as:

$$\frac{d\sigma}{dy_1 d^2p_{1t} dy_2 d^2p_{2t}} = \frac{1}{2\sigma_{eff}} \cdot \frac{d\sigma}{dy_1 d^2p_{1t}} \cdot \frac{d\sigma}{dy_2 d^2p_{2t}} \,. \tag{18}$$

The σ_{eff} parameter is in principle a free parameter responsible for the overlap of partonic densities of colliding protons. $\sigma_{eff} = 15$ mb is world average for different reactions. We shall use this value having in mind that a departure from the factorized Ansatz is possible. A complete calculation of the single parton scattering contributions should show how much room is left for the DPS contribution, which by itself is rather difficult to be calculated from first principle.

In Fig.18 we show mechanisms not included routinely in the calculation of simultaneous two J/ψ meson production. The first one (16 diagrams) was included before in [**?**] but was there not crucial. The second one was not discussed in the presentation at Epiphany, but will be presented soon elsewhere.

5.2. Selected results

Here we show some preliminary results obtained for very recent ATLAS data [13]. Both cuts on J/ψ and muon kinematical variables have been imposed. The details will be given elsewhere [9].

In Fig.19 we present distribution in rapidity difference between the two J/ψ mesons. Both the leading-order and two-gluon exchange contributions are shown for two different factorization scales. Summing the different contributions one can almost describe the experimental data except of very small rapidity differences. We ask the reader to note a similar shape of distributions for DPS and two-gluon exchange.

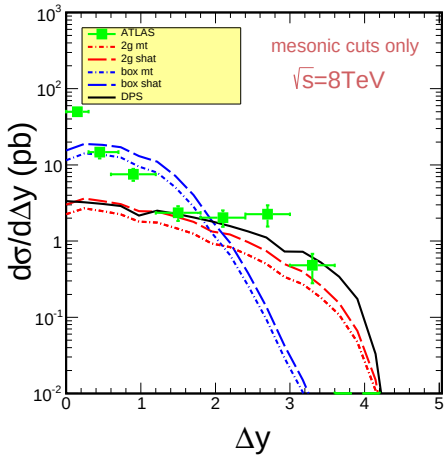


Fig. 19. Distribution in rapidity difference between the two J/ψ mesons. Contributions of different mechanisms are shown separately.

In Fig.20 we show distribution in dimeson invariant mass. In collinear-factorization approach and with the ATLAS experimental cuts on transverse momenta of J/ψ mesons there is a sharp cut off in meson invariant mass ($M > 20$ GeV). There is no such a sharp cut off for the DPS contributions where both J/ψ mesons are not correlated in azimuthal angle. Although we do not show the sum of the contributions it is obvious that no good description of the data is possible, especially for low invariant masses. This is will be discussed in detail in our forthcoming paper [9].

In collinear-factorization approach only $d\sigma/dy_{diff}$ and $d\sigma/dM_{VV}$ can be obtained. For the DPS mechanism also $p_{t,sum} = |\vec{p}_{1,t} + \vec{p}_{2,t}|$ distribution can be obtained as shown in Fig.21. Clearly the DPS contribution is not sufficient as can be seen by comparison of the cross section normalizations and in particular of the shapes of the theoretical and experimental distributions.

6. Conclusions

In the present paper we have discussed different reactions with the J/ψ meson in the final state.

We have started from exclusive $pp \to ppJ/\psi$ process. In contrast to other groups we include interference effect between the photon-pomeron and pomeron-photon amplitudes and present distributions in J/ψ transverse momentum. We have quantified the effect of including the anomalous

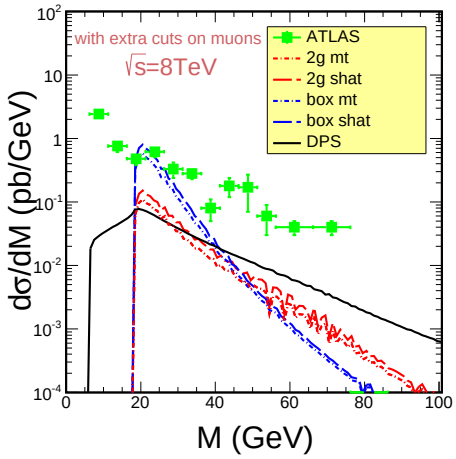


Fig. 20. Invariant mass distribution of two J/ψ mesons. Contributions of different mechanisms are shown separately.

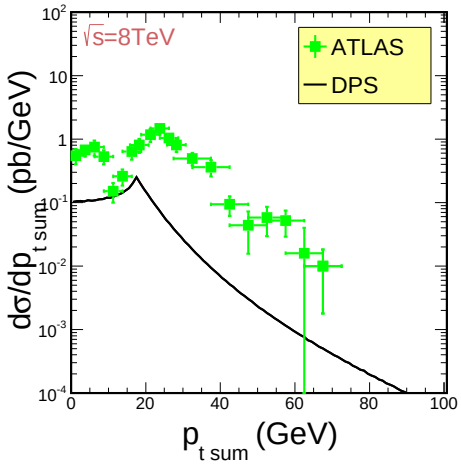


Fig. 21. Distribution of $p_{t,sum}$. Only the DPS contribution is shown and compared to the ATLAS data.

photon coupling to nucleon and those due to absorption effects, both often neglected in the literature. Our calculation suggest that the LHCb data show an onset of nonlinear effects.

However, some caution is required when interpreting the present experimental results. We have discussed that the present measurements were not fully exclusive as protons were not measured and only rapidity gap conditions were imposed experimentally. We have discussed the reaction in which one of the protons is dissociated, but large rapidity gaps around J/ψ are present. We called them semi-exclusive reactions. In general, there are two classes of the dissociative processes: associated with photon exchange and associated with pomeron exchange. We have presented a novel method to include electromagnetic dissociation. In this method the $p \to X$ vertex is expressed in terms of F_2 structure function. By using parametrizations valid in the full phase space one can include both resonance and continuum excitations. Diffractive excitations are more difficult to model. We have discussed both resonance contributions using a model from the literature and partonic continuum caused by the exchange of colour singlet two-gluon exchange with parameters adjusted to HERA data. We have shown that, in disagreement with naive expectation in the field, the electromagnetic excitation gives larger contribution than the diffractive one. The effect of the semiexclusive processes on rapidity and transverse momenta of the J/ψ mesons have been presented.

Paradoxically the inclusive production of J/ψ mesons is less understood than the exclusive one. Different authors have different opinions on the underlying mechanism. The difficulty is that the higher-order effects are more important than for other pQCD processes. In the present short review we have considered only so-called color-singlet mechanisms that, in contrast to color-octet mechanisms, can be calculated from first principles. To include higher order effects we have used the k_t-factorization method and modern unintegrated gluon distributions. In this presentation we have focused on the description of recent LHCb data for forwardly produced J/ψ mesons. Both direct and feed-down contributions were included. The rather forward production, especially for χ_c feed-down, is sensitive to small values of longitudinal momentum fraction. We have obtained a good description of lower energy rapidity distributions and gradually worse and worse description with increasing collisions energy when using the KMR UGDFs. Whether this a signal of nonlinear effects (saturation) is in our opinion still an open issue. We have shown that one can avoid the conflict with the LHCb experimental data using UGDFs that include nonlinear effects.

Finally we have addressed shortly the simultaneous production of two J/ψ mesons at intermediate transverse momenta. We have made calculation relevant for recent ATLAS data. Several mechanisms have been discussed. Several distributions have been shown. The leading (box) contribution was calculated in collinear approach. The double parton scattering was calculated using a data-driven approach using a simple parametrization of in-

clusive J/ψ data. It seems impossible to describe the new data with the two mechanisms. We have also presented results including the two-gluon exchange mechanism between two quark-antiquark fluctuations of gluons which turned out to be important at large rapidity difference between the two J/ψ mesons. Some plans for the future have been presented.

REFERENCES

[1] I. P. Ivanov, N. N. Nikolaev and A. A. Savin, Phys. Part. Nucl. **37** (2006) 1.

[2] A. Cisek, W. Schäfer and A. Szczurek, JHEP **1504** (2015) 159.

[3] W. Schäfer and A. Szczurek, Phys. Rev. **D76** (2007) 094014.

[4] A. Cisek, W. Schäfer and A. Szczurek, arXiv:1611.08210, in print in Phys. Lett. **B**.

[5] G. G. da Silveira, L. Forthomme, K. Piotrzkowski, W. Schäfer and A. Szczurek, JHEP **1502** (2015) 159 [arXiv:1409.1541 [hep-ph]].

[6] M. Łuszczak, W. Schäfer and A. Szczurek, Phys. Rev. D **93** (2016) no.7, 074018 [arXiv:1510.00294 [hep-ph]].

[7] A. Cisek and A. Szczurek, a paper in preparation.

[8] S. Baranov, private communication.

[9] A. Cisek, W. Schäfer and A. Szczurek, a paper in preparation.

[10] L. L. Jenkovszky, O. E. Kuprash, J. W. Lamsa, V. K. Magas and R. Orava, Phys. Rev. D **83** (2011) 056014 [arXiv:1011.0664 [hep-ph]].

[11] R. Fiore, L. L. Jenkovszky, F. Paccanoni and A. Prokudin, Phys. Rev. D **70** (2004) 054003 [hep-ph/0404021].

[12] B.A. Kniehl, D.V. Vasin, V.A. Saleev Phys. Rev. **D73** (2006) 074022.

[13] The ATLAS collaboration, arXiv:1612.02950.

[14] C.H. Kom, A. Kulesza and W.J. Stirling, Phys. Rev. Lett. **107** (2011) 082002.

[15] S.P. Baranov, A.M. Snigirev, N.P. Zotov, A. Szczurek and W. Schäfer, Phys. Rev. **D87** (2013) 034035.